# Isotopic Shift of Atom-Dimer Efimov Resonances in K-Rb Mixtures: Critical Effect of Multichannel Feshbach Physics

K. Kato,[1,*] Yujun Wang,[2,†] J. Kobayashi,[3] P. S. Julienne,[4] and S. Inouye[1]
[1]Graduate School of Science, Osaka City University, Sumiyoshi-ku, Osaka 558-8585, Japan
[2]Department of Physics, Kansas State University, 116 Cardwell Hall, Manhattan, Kansas 66506, USA
[3]Department of Physics, Graduate School of Science, Kyoto University, Kyoto 606-8502, Japan
[4]Joint Quantum Institute, University of Maryland and NIST, College Park, Maryland 20742, USA
(Received 25 October 2016; published 17 April 2017)

Multichannel Efimov physics is investigated in ultracold heteronuclear admixtures of K and Rb atoms. We observe a shift in the scattering length where the first atom-dimer resonance appears in the $^{41}$K-$^{87}$Rb system relative to the position of the previously observed atom-dimer resonance in the $^{40}$K-$^{87}$Rb system. This shift is well explained by our calculations with a three-body model including van der Waals interactions, and, more importantly, multichannel spinor physics. With only minor differences in the atomic masses of the admixtures, the shift in the atom-dimer resonance positions can be cleanly ascribed to the isolated and overlapping Feshbach resonances in the $^{40}$K-$^{87}$Rb and $^{41}$K-$^{87}$Rb systems, respectively. Our study demonstrates the role of multichannel Feshbach physics in determining Efimov resonances in heteronuclear three-body systems.

DOI: 10.1103/PhysRevLett.118.163401

If physical systems exhibit properties that are independent of the details of the interaction, they are called universal [1]. Universality has played a central role in the analysis of quantum degenerate gases; e.g., the effect of binary collisions were successfully characterized by a single parameter, the $s$-wave scattering length $a$, independent of the details of the two-body potential. For few-body phenomena, however, it has been well known that an additional parameter—e.g., a three-body parameter [1]—is necessary for a complete description of the system. Efimov states, an infinite series of three-body bound states with discrete scale invariance when a two-body scattering length diverges [2], provided us a unique opportunity to investigate the properties of the three-body parameter both theoretically and experimentally. Combined experimental efforts to observe Efimov-related resonances provided us with an unexpected constancy of three-body parameters [3–9], while detailed theoretical analysis showed the origin of this constancy in some limiting cases [10,11]. Recent topics of Efimov physics are reviewed in Ref. [12].

Recently, a three-body spinor model that included both van der Waals interactions and multichannel Feshbach physics was developed [13]. It was impressive to see that predictions from a three-body model constructed to reproduce only two-body Feshbach physics match almost perfectly with the experimentally observed three-body features in homonuclear systems [13,14]. This achievement suggests that the necessity of including precise few-body short-range chemical forces in studies of universal few-body phenomena—a task far beyond our current capability—may be removed.

Extending this universal theory to *heteronuclear* systems is the next big challenge. In addition to the mass ratio, heteronuclear systems have the extra complication of having both inter- and intraspecies scattering lengths. The predictions of the single-channel universal van der Waals theory [15] have been confirmed in experiments with several heteronuclear systems [16–19], and the effect of multichannel Feshbach physics has therefore not been well demonstrated and understood.

We focus on the systems with small or moderate mass ratios—the "Efimov-unfavored" systems, where the origin of universality is similar to homonuclear systems [15]. There are several experimental groups working on Efimov-unfavored systems of K-Rb admixtures [20–23]. We compare our experimental results for $^{41}$K-$^{87}$Rb mixture with those obtained by the JILA group for the $^{40}$K-$^{87}$Rb mixture [21,22]. In general, Efimov-unfavored systems have relatively small universal scaling constant $s_0$, which leads to the large Efimov scaling cycle $e^{\pi/s_0}$ [1]; the size of the scattering length needed for seeing an Efimov resonance in three-body recombination is too large to be realized experimentally. We therefore measure the positions of the Efimov-like atom-dimer resonances instead, which could be observed at significantly lower scattering length [24]. For a comprehensive analysis of the heteronuclear Efimov resonance, we also investigate the three-body loss in $^{41}$K-$^{87}$Rb admixtures. We confirmed the absence of resonance in a three-body recombination, which is consistent with the universal predictions [15].

These two K-Rb systems are suitable for comparing the single- and multichannel theories for Efimov physics. They are nearly identical in the single channel theory: the van der Waals lengths ($r_{\mathrm{vdW}}$) are $71.9a_0$ and $72.2a_0$ [25], where $a_0$ is the Bohr radius, and the scaling parameters $s_0$ for two Rb

 © 2017 American Physical Society

atoms and one K atom are 0.6444 and 0.6536, for the $^{41}$K-$^{87}$Rb and $^{40}$K-$^{87}$Rb mixtures, respectively [24]. However, they are different in multichannel theory: they exhibit different two-body Feshbach spectra, the overlapping resonances for the $^{41}$K-$^{87}$Rb mixture, and the isolated resonance for the $^{40}$K-$^{87}$Rb mixture. The description of these Feshbach resonances is summarized in Ref. [26]. We observed a shift of Efimov atom-dimer resonances in these isotopic systems. Our new spinor model successfully reproduced this result and this fact reveals the critical effect of multichannel Feshbach physics on the heteronuclear systems.

The details of our experimental setup can be found in Refs. [26,29]. In summary, we prepared a dual-species Bose-Einstein condensate (dual-BEC) comprising $^{41}$K and $^{87}$Rb atoms in a crossed optical dipole trap. Both atoms are in the $|F, m_F\rangle = |1, 1\rangle$ state, where $F$ corresponds to the atomic angular momentum and $m_F$ is its projection. The typical number of each of the $^{87}$Rb and $^{41}$K atoms in a dual BEC is $\sim 4 \times 10^4$.

When it comes to the study of inelastic atom-dimer collisions, it is necessary for dimers to be produced efficiently. This is especially true for a Bose-Bose mixture, in which a large contribution from atom-dimer and dimer-dimer inelastic collisions limits the efficiency with which the dimers in traps are produced. We resolve this problem by using a three-dimensional optical lattice. Some preparatory steps are needed before the dual-BEC can be loaded onto the optical lattice potential. First, we compensate for the differential gravitational sag between the $^{41}$K and $^{87}$Rb atoms by introducing an additional laser beam whose wavelength is 809 nm [30]. Second, we decompress the BEC by decreasing the trapping frequencies in the horizontal directions. This is necessary for increasing the number of lattice sites that have exactly one K and one Rb atom when they become a dual Mott insulator phase. Typical trap frequencies for K and Rb are $(f_x, f_y, f_z) = (13, 92, 38)$ and (10,92,38) Hz, respectively, where the $y$ axis is the axis of gravity. Finally, we set the magnetic field $B = 85$ G, where interspecies scattering length $a = -20a_0$. At this magnetic field, the dual BEC is miscible because the interspecies scattering length is much smaller than the intraspecies scattering length [$a_{\mathrm{KK}} = 63.5(6)a_0$ [31], $a_{\mathrm{RbRb}} = 100.4(1)a_0$ [32]].

As we raised the optical lattice potential, the dual BEC was transformed into a dual Mott insulator. Then magnetic field was swept across the Feshbach resonance at 78.82 G and the atoms were adiabatically associated into molecules. For measuring the atom(Rb)-dimer(KRb) loss coefficient, we selectively removed the K atoms [26]. Before absorption imaging, the atoms and molecules were spatially separated in the horizontal direction via application of a magnetic field gradient during the time of flight. Furthermore, molecules were dissociated into atoms by sweeping the magnetic field across Feshbach resonance. The typical numbers of Rb atoms and KRb molecules are $\sim 1.1 \times 10^4$ and $\sim 3 \times 10^3$, respectively.

The atom-dimer loss coefficient $\beta_{\mathrm{ad}}$ was determined by placing the atom-dimer mixture into a dipole trap and measuring the number of dimers and atoms after a variable holding time $t$. The rate equation for the number of dimers $N_{\mathrm{KRb}}$ can be expressed as follows:

$$\dot{N}_{\mathrm{KRb}}(t) = -\beta_{\mathrm{ad}} \int n_{\mathrm{Rb}}(\boldsymbol{r}, t) n_{\mathrm{KRb}}(r, t) d^3\boldsymbol{r} - 2\beta_{\mathrm{dd}} \int n_{\mathrm{KRb}}(\boldsymbol{r}, t)^2 d^3\boldsymbol{r}. \quad (1)$$

In this equation, $N_{\mathrm{KRb}}(t)$ is the number of KRb dimers; $n_{\mathrm{Rb}}(\boldsymbol{r}, t)$ and $n_{\mathrm{KRb}}(\boldsymbol{r}, t)$ are the densities of Rb atoms and KRb dimers, respectively; and $\beta_{\mathrm{ad}}$ and $\beta_{\mathrm{dd}}$ are the loss coefficients for the atom-dimer and dimer-dimer collisions, respectively. Assuming a thermal distribution for the atoms and dimers in the dipole trap, the right-hand side of Eq. (1) can be calculated using the number and temperature of atoms and dimers from the time-of-flight images. Both $\beta_{\mathrm{ad}}$ and $\beta_{\mathrm{dd}}$ can be evaluated by comparing the experimental data from different initial conditions [26]. Figure 1 shows the measured atom-dimer and dimer-dimer loss coefficient, $\beta$. The magnetic field was converted into the scattering length by using the $a(B)$ from our multichannel two-body calculation. The calculation uses the atomic potentials in Refs. [33,34] and is calibrated carefully to give the correct positions of the Feshbach resonances. The dimer-dimer loss coefficient $\beta_{\mathrm{dd}}(a)$ does not show any prominent features [26]. The resonant feature was clearly observed in the atom-dimer loss coefficient $\beta_{\mathrm{ad}}(a)$, and the overall shape of the resonance was

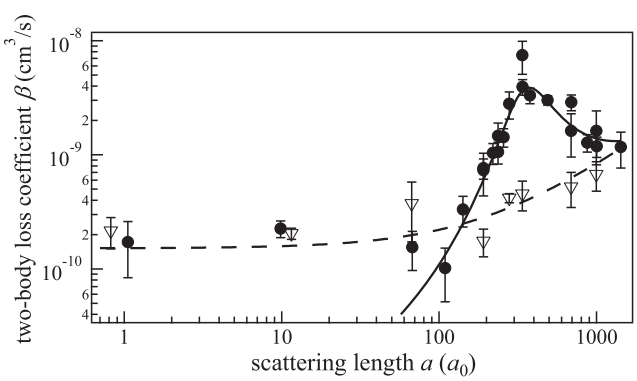


FIG. 1. Atom-dimer and dimer-dimer loss coefficients observed in an ultracold $^{41}$K-$^{87}$Rb system. While the dimer-dimer (KRb-KRb) loss coefficient (open triangles) does not show any prominent features, the atom-dimer (Rb-KRb) loss coefficient (circles) shows a resonant feature. Lines of best fit for dimer-dimer and atom-dimer loss coefficients are illustrated by dashed and solid lines. The fit for the dimer-dimer loss coefficient assumes a linear dependence on $a$, while the fit for the atom-dimer loss assumes Eq. (2). The typical densities of the atoms and dimers are $n_{\mathrm{Rb}} = 1.3 \times 10^{11}$ and $n_{\mathrm{KRb}} = 0.7 \times 10^{11}$ cm$^{-3}$, respectively. The typical temperature is 60 nK.

TABLE I. Experimental results of the atom-dimer resonances for Rb + $^{41}$KRb and Rb + $^{40}$KRb collisions. These values are determined by fitting of Eq. (2). Subscripts of syst and fit denote systematic error and fitting error, respectively.

| | $a_*$ ($a_0$) | $\eta_*$ | $C_\beta$ |
|---|---|---|---|
| $^{41}$K-$^{87}$Rb | $348(8)_{\rm fit}(41)_{\rm syst}$ | $0.24(2)_{\rm fit}$ | $15.5(7)_{\rm fit}$ |
| $^{40}$K-$^{87}$Rb [21] | $230(10)_{\rm fit}(30)_{\rm syst}$ | $0.26(3)_{\rm fit}$ | $3.2(2)_{\rm fit}$ |

quite similar to that of the $^{87}$Rb-$^{40}$K$^{87}$Rb mixture. The peak position, however, was different. We can quantify the difference in the peak positions by fitting the curves with the results obtained from the effective field theory, which includes three fitting parameters ($a_*$, $\eta_*$, $C_\beta$) [35],

$$\beta_{\rm ad}(a) = C_\beta \frac{\sinh(2\eta_*)}{\sin^2[s_0 \ln(a/a_*)] + \sinh^2(\eta_*)} \frac{\hbar a}{m_1}. \quad (2)$$

In Eq. (2), $a_*$ represents the resonance position, $\eta_*$ is the resonance width, and $C_\beta$ is the overall magnitude of the loss. Note that $m_1$ is the mass of the K atom in this case, and $s_0$ is the scaling parameter. We can fit $\beta_{\rm ad}$ using Eq. (2) and compare the results with those obtained for the $^{40}$K-$^{87}$Rb system. The results of both fits are summarized in Table I.

An isotopic comparison showed that $\eta_*$ matches within the error bars, while $a_*$ and $C_\beta$ are different between the two isotopes. The difference in $C_\beta$ can be attributed to the systematic uncertainty in density calibration, whereas the difference in $a_*$ [36] signifies the difference in the position of the peak. Thus, it is worth asking whether the difference can be attributed to the difference of the properties of the Feshbach resonances.

To better understand why there was an isotopic difference, we also checked the three-body recombination rate. Recent studies on the three-body recombination coefficient of the K-Rb systems [21–23] showed that there is no Efimov-related resonance in the region of $200a_0 < |a| < 3000a_0$. Furthermore, the single-channel universal theory on the heteronuclear Efimov resonance for broad resonance predicts that there is no resonance in the region of $|a| < 2800a_0$ [15].

Experimental details on how the three-body loss coefficient was measured are presented in Ref. [26]. Measuring the three-body loss coefficient for a heteronuclear system of bosonic atoms is problematic because we have to distinguish between competing processes. In the case of the three-body loss for the $^{41}$K-$^{87}$Rb mixture in the vicinity of the $^{41}$K-$^{87}$Rb Feshbach resonance, there are two major contributions: K-K-Rb and K-Rb-Rb [26]. Therefore, increasing the signal-to-noise ratio of data is mandatory. In our experiment, the main source of noise in the data analysis originated from fluctuations in the initial number of atoms. We eliminated these fluctuations by taking multiple images of the same cloud using phase-contrast imaging. Additionally, we enhanced the three-body loss by increasing the atomic density [26]. The measured three-body recombination loss coefficients are shown in Fig. 2. In the vicinity of resonance, three-body recombination loss coefficient deviates from the $a^4$ dependence and shows saturation. In general, saturation can be caused by either temperature [37,38] or density [39]. In this experiment, the typical density, temperature, and phase-space density of the gas were approximately $1 \times 10^{13}$ cm$^{-3}$, 400 nK, and 0.5, respectively. Since the phase-space density was high, the saturation of the loss coefficient was dominated by the density effect [which happens when the scattering length reaches the interparticle spacing $k^{-1} = 1/(6\pi^2 n)^{1/3} = 2000a_0$] rather than the temperature effect (which happens when the scattering length approaches the thermal de Broglie length $\lambda_{\rm dB} = 6000a_0$). The saturation was clearly observed in the negative side of the three-body loss coefficient. What is happening on the positive side is less clear. Again, it could be just the saturation, but we cannot exclude the possibility of three-body loss coefficient having a minimum in $a > 1300a_0$ region. Note that the absolute value of the three-body recombination loss coefficient is smaller than the previously reported value [23]. We believe this discrepancy comes from the fact that we did a complete analysis by including the other loss channel (i.e., K-K-Rb) [26] that was neglected in Ref. [23].

The significant shift in the positions of the atom-dimer resonances in the two isotopic K-Rb admixtures clearly

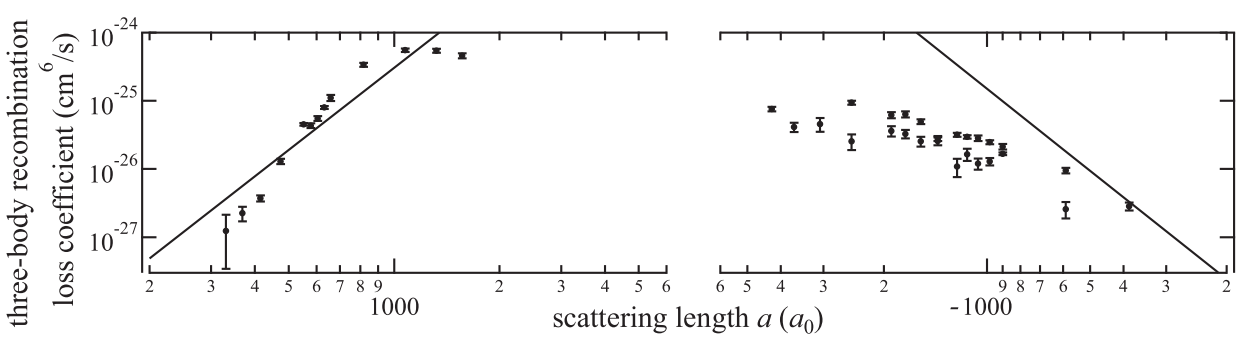


FIG. 2. The three-body recombination loss coefficient of the K-Rb-Rb collision in the vicinity of the heteronuclear Feshbach resonance (circles). The solid line shows an $a^4$ dependence, and the amplitude factor is determined by a fitting on the range of the positive scattering length $200a_0 < a < 1300a_0$. On the negative side, the amplitude factor is half of its value on the positive side [24].

cannot be explained by the small differences in the van der Waals lengths or the universal scaling constants. In fact, the single-channel, universal van der Waals three-body theory fails here by a large margin with an incorrectly predicted atom-dimer resonance near $a = 100a_0$. The failure of the universal theory raises the important question of whether the general universality, i.e., the independence of Efimov physics on short-range chemical forces, is still valid.

Our approach to address the above question is to perform three-body calculations with a spinor model that reproduces the relevant two-body Feshbach spectra in each of the isotopic systems. Such a model is relatively easy to build in the Rb-Rb-K system because the multichannel physics is only important for the K-Rb pairs, whereas a single-channel description is a good approximation for the Rb-Rb interaction in the whole range of the magnetic field of our current interest. Our theory, therefore, allows the K atom to carry the (pseudo)spin degrees of freedom and treats Rb atoms as spinless. Specifically, the total three-body wave function $\Psi$ is expanded as $\Psi = \sum_\alpha \psi_\alpha |\alpha\rangle$, where $|\alpha\rangle$ is the (pseudo)spin state of the K atom.

With the spinor model, we solve the three-body Schrödinger equation in the form of

$$(T + V_{\mathrm{RbRb}})\psi_\alpha + \sum_\beta (V^{(\alpha\beta)}_{\mathrm{KRb},1} + V^{(\alpha\beta)}_{\mathrm{KRb},2})\psi_\beta = (E - \epsilon_\alpha)\psi_\alpha, \tag{3}$$

where $T$ is the three-body kinetic energy operator; $V_{\mathrm{RbRb}}$, $V^{(\alpha\beta)}_{\mathrm{KRb},1}$, and $V^{(\alpha\beta)}_{\mathrm{KRb},2}$ are the single- and multichannel two-body potentials of the three pairs of the atoms; and $\epsilon_\alpha$ is the single-atom energy level of the K atom. The proper magnetic-field dependence of the three-body Hamiltonian is built in the single-atom energy as $\epsilon_\alpha = \mu_\alpha B + u_\alpha$, where the magnetic moment $\mu_\alpha$ and the zero-field energy $u_\alpha$ are chosen to mimic the realistic magnetic moments and the hyperfine splittings [26]. We solve Eq. (3) and calculate the atom-dimer loss coefficients with essentially the same potential models and numerical techniques used in Ref. [13].

In Figure 3 we show our numerically calculated atom-dimer loss rates compared with the data from our and JILA's experiments. To properly reproduce the isolated and overlapping characters of the Feshbach resonances in $^{40}$K-Rb and $^{41}$K-Rb pairs, two-spin-state and three-spin-state model interactions are used for $V^{(\alpha\beta)}_{\mathrm{KRb}}$ in the $^{40}$K-Rb-Rb and $^{41}$K-Rb-Rb calculations, respectively. The results of these models are multiplied by 5 and 2, which are thermally averaged at 70 and 300 nK for Rb + $^{41}$KRb and Rb + $^{40}$KRb loss coefficients, respectively. The peak positions of the theoretical curves are $395a_0$ and $222a_0$ for Rb + $^{41}$KRb and Rb + $^{40}$KRb, respectively. We also calculated loss coefficients at different temperatures. A factor of 2 change in the temperature gives changes in the peak positions within $\pm 5a_0$ and $\pm 2a_0$ for Rb + $^{41}$KRb and Rb + $^{40}$KRb systems, respectively. Without fitting parameters, the calculated

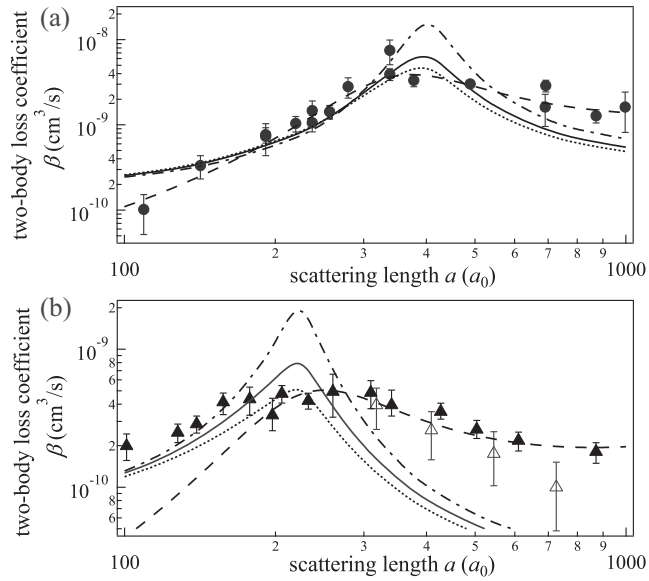


FIG. 3. Comparisons of numerically calculated and experimentally measured loss coefficients for (a) Rb + $^{41}$KRb and (b) Rb + $^{40}$KRb (experimental data obtained from Ref. [21]) collisions. In (a), the numerical results are multiplied by 5, which are thermally averaged at 20, 70, and 150 nK (dashed-dotted line, solid line, and dotted line). In (b), the numerical results are multiplied by 2, which are thermally averaged at 100, 300, and 500 nK (dashed-dotted line, solid line, and dotted line). In both graphs, results from numerical calculations at middle temperatures (shown in solid lines) show reasonable agreement with experimental results (shown in circles and triangles). The results from the fit using the effective field theory (dashed line) are also shown. The temperature of each measurement was ~60 (solid circles), ~150 (open triangles), and ~300 nK (solid triangles), respectively.

atom-dimer resonance positions agree well with both of the experimentally observed positions, and, consequently, reproduce the atom-dimer resonance shift in the isotopic systems. The need to scale the magnitude by a factor of 5 can be explained by the large uncertainty in atomic density in our experiment. On the other hand, there is also limited predictability on the absolute magnitude of the atom-dimer loss rates from theory. The absolute magnitudes of the atom-dimer loss rates are susceptible to the low-lying atom-dimer decay channels. We expect the overall magnitude is predicted within a factor of about 2. Note that the character of the resonant features in the calculations, in particular the positions of the resonance—the main topic of our current study—is generally unaffected by the change in the overall magnitudes.

For the $^{41}$K-Rb-Rb system, we point out that in order to correctly predict the atom-dimer resonance position, it is necessary for the three-body model to reproduce both the background (39) and overlapping (79 G) Feshbach resonances. A model that reproduces only the local properties of the overlapping resonance does not give the atom-dimer resonance position correctly. Another observation is that regardless of the number of spin states, the calculated loss

rates in the two isotopic systems have similar magnitude when the scattering length is low. This suggests that the observed shift of the atom-dimer resonance position—going beyond the single-channel van der Waals theory—is the manifestation of the difference in the underlying two-body Feshbach physics. The short-range chemical forces are clearly not involved.

In summary, we measured the heteronuclear atom-dimer loss coefficients of $^{87}$Rb atoms and $^{41}$K$^{87}$Rb Feshbach molecules at ultracold temperatures. The observed loss coefficient showed an Efimov-related resonance at $a_* = 348(8)_{\rm fit}(41)_{\rm syst}\, a_0$, which shifted from previous measurements for different isotopes of potassium. To explain this shift, we modeled the system using a three-body spinor theory that reproduced the properties of Feshbach resonances. This theory was successful in reproducing the experimental results of the atom-dimer resonance for both isotopes. These results show the important role of the multichannel Feshbach physics in shifting the positions of the three-body Efimov resonances, and demonstrate the independence of these three-body resonances from short-range chemical forces in the heteronuclear atomic systems even near relatively narrow Feshbach resonances.

The authors would like to thank Shimpei Endo and Pascal Naidon for their valuable suggestions. This work was supported by JSPS KAKENHI Grant-in-Aid for Scientific Research(B), Grant No. JP23340117.

*k_kato@sci.osaka-cu.ac.jp
†Present address: American Physical Society, 1 Research Road, Ridge, New York 11961, USA.

[1] E. Braaten and H.-W. Hammer, Phys. Rep. **428**, 259 (2006).
[2] V. Efimov, Phys. Lett. B **33**, 563 (1970).
[3] T. Kraemer, M. Mark, P. Waldburger, J. G. Danzl, C. Chin, B. Engeser, A. D. Lange, K. Pilch, A. Jaakkola, H. C. Nägerl, and R. Grimm, Nature (London) **440**, 315 (2006).
[4] M. Zaccanti, B. Deissler, C. D'rrico, M. Fattori, M. Jona-Lasinio, S. Müller, G. Roati, M. Inguscio, and G. Modugno, Nat. Phys. **5**, 586 (2009).
[5] A. N. Wenz, T. Lompe, T. B. Ottenstein, F. Serwane, G. Zürn, and S. Jochim, Phys. Rev. A **80**, 040702 (2009).
[6] N. Gross, Z. Shotan, S. Kokkelmans, and L. Khaykovich, Phys. Rev. Lett. **103**, 163202 (2009).
[7] M. Berninger, A. Zenesini, B. Huang, W. Harm, H.-C. Nägerl, F. Ferlaino, R. Grimm, P. S. Julienne, and J. M. Hutson, Phys. Rev. Lett. **107**, 120401 (2011).
[8] R. J. Wild, P. Makotyn, J. M. Pino, E. A. Cornell, and D. S. Jin, Phys. Rev. Lett. **108**, 145305 (2012).
[9] P. Dyke, S. E. Pollack, and R. G. Hulet, Phys. Rev. A **88**, 023625 (2013).
[10] J. Wang, J. P. D'Incao, B. D. Esry, and C. H. Greene, Phys. Rev. Lett. **108**, 263001 (2012).
[11] P. Naidon, S. Endo, and M. Ueda, Phys. Rev. A **90**, 022106 (2014).
[12] P. Naidon and S. Endo, arXiv:1610.09805.
[13] Y. Wang and P. S. Julienne, Nat. Phys. **10**, 768 (2014).
[14] A. Zenesini, B. Huang, M. Berninger, H.-C. Nägerl, F. Ferlaino, and R. Grimm, Phys. Rev. A **90**, 022704 (2014).
[15] Y. Wang, J. Wang, J. P. D'Incao, and C. H. Greene, Phys. Rev. Lett. **109**, 243201 (2012).
[16] S.-K. Tung, K. Jiménez-García, J. Johansen, C. V. Parker, and C. Chin, Phys. Rev. Lett. **113**, 240402 (2014).
[17] R. Pires, J. Ulmanis, S. Häfner, M. Repp, A. Arias, E. D. Kuhnle, and M. Weidemüller, Phys. Rev. Lett. **112**, 250404 (2014).
[18] J. Ulmanis, S. Häfner, R. Pires, E. D. Kuhnle, Y. Wang, C. H. Greene, and M. Weidemüller, Phys. Rev. Lett. **117**, 153201 (2016).
[19] R. A. W. Maier, M. Eisele, E. Tiemann, and C. Zimmermann, Phys. Rev. Lett. **115**, 043201 (2015).
[20] G. Barontini, C. Weber, F. Rabatti, J. Catani, G. Thalhammer, M. Inguscio, and F. Minardi, Phys. Rev. Lett. **103**, 043201 (2009).
[21] R. S. Bloom, M.-G. Hu, T. D. Cumby, and D. S. Jin, Phys. Rev. Lett. **111**, 105301 (2013).
[22] M.-G. Hu, R. S. Bloom, D. S. Jin, and J. M. Goldwin, Phys. Rev. A **90**, 013619 (2014).
[23] L. J. Wacker, N. B. Jørgensen, D. Birkmose, N. Winter, M. Mikkelsen, J. Sherson, N. Zinner, and J. J. Arlt, Phys. Rev. Lett. **117**, 163201 (2016).
[24] K. Helfrich, H.-W. Hammer, and D. S. Petrov, Phys. Rev. A **81**, 042715 (2010).
[25] A. Simoni, M. Zaccanti, C. D'Errico, M. Fattori, G. Roati, M. Inguscio, and G. Modugno, Phys. Rev. A **77**, 052705 (2008).
[26] See Supplemental Material at http://link.aps.org/supplemental/10.1103/PhysRevLett.118.163401, which includes Refs. [27,28], for details of the interaction models in three-body calculations and sample preparation for each loss measurement.
[27] B. P. Ruzic, C. H. Greene, and J. L. Bohn, Phys. Rev. A **87**, 032706 (2013).
[28] J. Söding, D. Guéry-Odelin, P. Desbiolles, F. Chevy, H. Inamori, and J. Dalibard, Appl. Phys. B **69**, 257 (1999).
[29] T. Kishimoto, J. Kobayashi, K. Noda, K. Aikawa, M. Ueda, and S. Inouye, Phys. Rev. A **79**, 031602 (2009).
[30] S. Ospelkaus-Schwarzer, Ph. D. thesis, Universität Hamburg, 2006.
[31] S. Falke, H. Knöckel, J. Friebe, M. Riedmann, E. Tiemann, and C. Lisdat, Phys. Rev. A **78**, 012503 (2008).
[32] E. G. M. van Kempen, S. J. J. M. F. Kokkelmans, D. J. Heinzen, and B. J. Verhaar, Phys. Rev. Lett. **88**, 093201 (2002).
[33] A. Pashov, O. Docenko, M. Tamanis, R. Ferber, H. Knöckel, and E. Tiemann, Phys. Rev. A **76**, 022511 (2007).
[34] C. Klempt, T. Henninger, O. Topic, J. Will, W. Ertmer, E. Tiemann, and J. Arlt, Phys. Rev. A **76**, 020701 (2007).
[35] This form is expected to be valid when $a > 2r_{\rm vdW}$ [24]
[36] The systematic error of $a_*$ comprises a fluctuation in the magnetic field and the uncertainty of $a$-to-B conversion.
[37] B. S. Rem, A. T. Grier, I. Ferrier-Barbut, U. Eismann, T. Langen, N. Navon, L. Khaykovich, F. Werner, D. S. Petrov, F. Chevy, and C. Salomon, Phys. Rev. Lett. **110**, 163202 (2013).
[38] D. S. Petrov and F. Werner, Phys. Rev. A **92**, 022704 (2015).
[39] P. Makotyn, C. E. Klauss, D. L. Goldberger, E. A. Cornell, and D. S. Jin, Nat. Phys. **10**, 116 (2014).